Inorg. Chem. **2002**, *41*, 121–126

Chalcogen Rich Lanthanide Clusters from Halide Starting Materials (II): Selenido Compounds

Anna Kornienko, J. H. Melman, G. Hall, T. J. Emge, and John G. Brennan*

Department of Chemistry, Rutgers, the State University of New Jersey, 610 Taylor Road, Piscataway, New Jersey 08854-8087

Received July 11, 2001

Lanthanides reduce mixtures of I_2 and PhSeSePh in THF, and the resultant heteroligand mixture reacts further with elemental Se in pyridine to give $(THF)_6Ln_4I_2(SeSe)_4(\mu_4\text{-Se})\cdot THF$ (Ln = Tm, Ho, Er, Yb). These selenium rich clusters contain a square array of Ln(III) ions connected through a single (μ_4-Se) ligand. There are two I^- ligands coordinating nonadjacent Ln(III) ions on the side of the cluster opposite the (μ_4-Se), and the edges of the square are bridged by μ_2-SeSe groups. The electronic spectrum of the Yb compound contains two absorption maxima that can tentatively be assigned as Se^{2-} to Yb and SeSe to Yb charge-transfer absorptions, by comparison with the featureless absorption spectra of the Tm, Ho, and Er derivatives. With a 1/1/1/1 Yb/I/Ph_2S_2/Se stoichiometry, chalcogen rich compounds are not obtained, but instead, in Yb chemistry, the selenido cluster $(THF)_{10}Yb_6Se_6I_6$ can be isolated in 51% yield. The molecular structure of this compound contains a Yb_4Se_4 cubane fragment, with an additional Yb_2Se_2 layer capping one face of the cube. Each Yb coordinates a terminal I^-. This intensely colored compound also has an absorption maximum in the visible spectrum. Upon thermolysis, the selenium rich compounds give Ln_2Se_3 that is free of iodide contamination.

Introduction

Recent interest in lanthanide (Ln; Ln = La−Lu) compounds with only chalcogen (E; E = S, Se, or Te) based anionic ligands continues to be motivated both by a fundamental interest in the nature of the Ln−E bond and by the potential applications of Ln ions in chalcogenido based pigments[1] and optical fibers.[2] Only in the past decade, with the synthesis of $Ln(ER)_x$ (R = organic; x = 2, 3) compounds,[3] has it become apparent that highly electronegative, sterically saturating ancillary ligands[4] (e.g., Cp*) are not a prerequisite for the successful isolation and characterization of molecular compounds with Ln−E bonds.

Chalcogenido (E^{2-}) cluster chemistry of the lanthanides is less well developed. The most general synthetic approach to these materials involves the reduction of elemental E by $Ln(EPh)_3$, with concomitant oxidative elimination of PhEEPh.[5] This reactivity has been controlled to give crystalline homo- and heterometallic clusters, heterovalent compounds, and clusters with most combinations of Ln, E, EPh, and neutral

* Author to whom correspondence should be addressed. E-mail: bren@rutchem.rutgers.edu.

(1) (a) Macaudiere, P. U.S. Patent 5,968,247, 1999. (b) Chopin, T.; Guichon, H.; Touret, O. U.S. Patent 5,348,581, 1994. (c) Chopin, T.; Dupuis, D. U.S. Patent 5,401,309, 1995.

(2) (a) Tawarayama, H.; Ishikawa, E.; Toratani, H. *J. Am. Ceram. Soc.* **2000**, *83*, 792. (b) Griscom, L. S.; Adam, J.-L.; Binnemans, K. *J. Non-Cryst. Solids* **1999**, *256/257*, 383. (c) Choi, Y. G.; Kim, K. H.; Heo, J. *J. Appl. Phys.* **2000**, *88*, 3832. (d) Shin, Y. B.; Heo, J.; Kim, H. S. *Chem. Phys. Lett.* **2000**, *317*, 637. (e) Choi, Y. G.; Kim, K. H.; Heo, J. J. *Appl. Phys. Lett.* **2001**, *78*, 1249. (f) Cole, B.; Shaw, L. B.; Aggarwal, I. D. *J. Non-Cryst. Solids* **1999**, *256/257*, 253. (g) Adam, J.-L.; Doualan, J.-L.; Moncorge, R. *J. Non-Cryst. Solids* **1999**, *256/257*, 276. (h) Furniss, D.; Seddon, A. B. *J. Mater. Sci. Lett.* **1998**, *17*, 1541. (i) Harbison, B. B.; Sanghera, J. S.; Shaw, L. B.; Aggarwal, I. D. U.S. Patent 6,015,765, 2000.

(3) (a) Nief, F. *Coord. Chem. Rev.* **1998**, *178−80*, 13. (b) Lee, J.; Freedman, D.; Melman, J.; Brewer, M.; Sun, L.; Emge, T. J.; Long, F. H.; Brennan, J. G. *Inorg. Chem.* **1998**, *37*, 2512. (c) Freedman, D.; Kornienko, A.; Emge, T.; Brennan, J. G. *Inorg. Chem.* **2000**, *39*, 2168. (d) Melman, J.; Emge, T.; Brennan, J. G. *Inorg. Chem.* **2001**, *40*, 1078.

(4) (a) Schumann, H.; Albrecht, I.; Hahn, E. *Angew. Chem., Int. Ed. Engl.* **1985**, *24*, 985. (b) Berg, D.; Burns, C.; Andersen, R. A.; Zalkin, A. *Organometallics* **1988**, *7*, 1858. (c) Berg, D. J.; Burns, C.; Andersen, R. A.; Zalkin, A. *Organometallics* **1989**, *8*, 1865. (d) Zalkin, A.; Berg, D. J. *Acta Crystallogr.* **1988**, *44C*, 1488−1489. (e) Evans, W.; Grate, J. W.; Bloom, I.; Hunter, W. E.; Atwood, J. L. *J. Am. Chem. Soc.* **1985**, *107*, 405. (f) Evans, W.; Rabe, G.; Ziller, J.; Doedens, R. *Inorg. Chem.* **1994**, *33*, 2719. (g) Welder, M.; Noltemeyer, M.; Pieper, U.; Schmidt, H.; Stalke, D.; Edelmann, F. *Angew. Chem., Int. Ed. Engl.* **1990**, *29*, 894.

(5) (a) Freedman, D.; Emge, T. J.; Brennan, J. G. *J. Am. Chem. Soc.* **1997**, *119*, 11112. (b) Melman, J. H.; Emge, T. J.; Brennan, J. G. *Chem. Commun.* **1997**, 2269. (c) Melman, J. H.; Emge, T. J.; Brennan, J. G. *Inorg. Chem.* **1999**, *38*, 2117. (d) Freedman, D.; Emge, T. J.; Brennan, J. G. *Inorg. Chem.* **1999**, *38*, 4400. (e) Freedman, D.; Melman, J. H.; Emge, T. J.; Brennan, J. G. *Inorg. Chem.* **1998**, *37*, 4162. (f) Freedman, D.; Safik, S.; Emge, T. J.; Croft, M.; Brennan, J. G. *J. Am. Chem. Soc.* **1999**, *121*, 11713.

10.1021/ic010740o CCC: $22.00
Published on Web 12/14/2001

donor ligands, usually in high yields. The cubic octanuclear array of Ln ions in the $Ln_8E_6(EPh)_{12}$ series is observed for most Ln (Ce−Er),[5a−d] while the smaller Ln (Tm, Yb) tend to form clusters with cubane[5e] based geometries. Because the structural, magnetic, and electronic properties of the molecular chalcogenolate compounds were well understood, the corresponding cluster properties were readily interpreted.

As single source precursors to solid-state materials, these molecular chalcogenolates and chalcogenido cluster compounds have one significant flaw: thermal decomposition relies on a long known thermolytic pathway[6] involving cleavage of an E−C bond and the elimination of RER. Unfortunately, E−C cleavage reactions invariably trap organic residues in the thermolysis product, and useful electronic materials rarely tolerate significant impurity levels. The recent isolation and structural characterization of $(THF)_6Yb_4I_2(SS)_4(\mu_4\text{-S})$ represented the first single source precursor to solid-state LnE_x that did not require elimination of RER. Thermolysis of this compound gave LnS_x that was both free of carbon contamination and significant iodide incorporation.[7] Here, we describe our initial investigations into the halogenated cluster chemistry of the $LnSe_x$ system, including the first halogenated lanthanide cubane.

Experimental Section

General Methods. All syntheses were carried out under ultrapure nitrogen (JWS), using conventional drybox or Schlenk techniques. Solvents (Fisher) were refluxed continuously over molten alkali metals or K/benzophenone and collected immediately prior to use. Anhydrous pyridine was purchased from Aldrich and refluxed over KOH. PhSeSePh and PhSSPh were purchased from Aldrich and recrystallized from hexane. Ln and Hg were purchased from Strem. Melting points were taken in sealed capillaries and are uncorrected. IR spectra were taken on a Mattus Cygnus 100 FTIR spectrometer and recorded from 4000 to 600 cm^{-1} as a Nujol mull on NaCl plates. Electronic spectra were recorded on a Varian DMS 100S spectrometer with the samples in a 0.10 mm quartz cell attached to a Teflon stopcock. Elemental analyses were performed by Quantitative Technologies, Inc. (Whitehouse NJ). These compounds are sensitive to the thermal dissociation of neutral donor ligands at room temperature. X-ray powder diffraction spectra were obtained on a SCINTAG PAD V diffractometer with Cu Kα radiation. X-ray fluorescence measurements were obtained with an EDAX DX-95 energy dispersive spectrometer with Rh tube excitation operated at 30 kV and a current of 100 μA.

Synthesis of $(THF)_6Yb_4I_2(SeSe)_4(\mu_4\text{-Se})\cdot THF$ (1). Yb (346 mg, 2.0 mmol), diphenyl diselenide (780 mg, 2.5 mmol), iodine (127 mg, 0.5 mmol), and Hg (50 mg, 0.25 mmol) were combined in THF (50 mL). The mixture was stirred until all the metal was consumed to give a red solution with some red precipitate. Elemental Se powder (355 mg, 4.5 mmol) was added, and after 2 days, the deep red solution was filtered, concentrated to 30 mL, and layered with hexanes (10 mL) to give red crystals (343 mg, 32%) that do not melt but turn dark brown at 225 °C. Anal. Calcd for $C_{28}H_{56}O_7I_2Se_9Yb_4$: C, 15.6; H, 2.61. Found: C, 15.6; H, 2.72. UV−vis (THF): λ_{max} = 387 nm (425 L $mol^{-1}cm^{-1}$). IR: 3166 (s), 2877 (w), 2728 (m), 2670 (s), 2423 (s), 2361 (s), 2342 (s), 2206 (s), 2037 (s), 1903 (s), 1788 (s), 1670 (s), 1642 (m), 1460 (w), 1377 (w), 1316 (m), 1261 (s), 1168 (s), 1156 (s), 1097 (s), 1076 (s), 1035 (s), 1007 (m), 917 (s), 848 (s), 805 (s), 772 (s), 723 (m) cm^{-1}.

Synthesis of $(THF)_6Tm_4\ I_2(SeSe)_4(\mu_4\text{-Se})\cdot THF$ (2). Tm (338 mg, 2.0 mmol), diphenyl diselenide (780 mg, 2.5 mmol), iodine (127 mg, 0.5 mmol), and Hg (50 mg, 0.25 mmol) were mixed in THF (50 mL). The mixture was stirred until all the metal was consumed to give a yellow solution. Elemental Se (355 mg, 4.5 mmol) was added, and after 2 days, the mixture was filtered to remove a small amount of yellow precipitate. The orange solution was concentrated to ∼30 mL and layered with hexanes (10 mL) to give yellow crystals (0.19 g, 19%) that do not melt but turn dark brown at 210 °C. Anal. Calcd for $C_{28}H_{56}O_7I_2Se_9Tm_4$: C, 15.7; H, 2.63. Found: C, 17.1; H, 2.74. The compound does not show an optical absorption maximum from 300 to 800 nm in THF or pyridine. IR: 3165 (s), 2879 (w), 2724 (m), 2670 (s), 2401 (s), 2343 (s), 2174 (s), 2033 (s), 1751 (s), 1461 (w), 1377 (w), 1306 (m), 1262 (s), 1208 (s), 1155 (s), 1065 (s), 1036 (s), 1007 (m), 673 (s), 918 (s), 852 (s), 801 (s), 772 (s), 722 (m), 608 (s) cm^{-1}.

Synthesis of $(THF)_6Er_4I_2(SeSe)_4(\mu_4\text{-Se})\cdot THF$ (3). As for **2**, Er (334 mg, 2.0 mmol), diphenyl diselenide (780 mg, 2.5 mmol), iodine (127 mg, 0.5 mmol), and Hg (50 mg, 0.25 mmol) in THF (50 mL), followed by Se powder (355 mg, 4.5 mmol), gave yellow crystals (0.21 g, 20%) that do not melt but turn dark brown at 245 °C. Anal. Calcd for $C_{28}H_{56}O_7I_2Se_9Er_4$: C, 15.7; H, 2.64. Found: C, 15.7; H, 2.59. The compound does not show an optical absorption maximum from 300 to 800 nm in THF or pyridine. IR: 3163 (s), 2895 (w), 2724 (m), 2670 (s), 2362 (s), 2343 (s), 2153 (s), 2021 (s), 1719 (s), 1655 (s), 1543 (s), 1461 (w), 1377 (w), 1306 (m), 1260 (s), 1208 (s), 1156 (s), 1063 (s), 1036 (s), 1004 (m), 917 (s), 852 (s), 805 (s), 772 (s), 723 (m), 608 (s) cm^{-1}.

Synthesis of $(THF)_6Ho_4I_2(SeSe)_4(\mu_4\text{-Se})\cdot THF$ (4). As for **2**, Ho (330 mg, 2.0 mmol), diphenyl diselenide (780 mg, 2.5 mmol), iodine (127 mg, 0.5 mmol), and Hg (50 mg, 0.25 mmol) in THF (50 mL), followed by Se powder (356 mg, 4.5 mmol), gave yellow crystals (0.265 g, 25%) that do not melt but turn dark brown at 189 °C. Anal. Calcd for $C_{28}H_{56}O_7I_2Se_9Ho_4$: C, 15.8; H, 2.65. Found: C, 15.3; H, 2.74. The compound does not show an optical absorption maximum from 300 to 800 nm in THF or pyridine. IR: 3165 (s), 2925(w), 2869 (w), 2727 (m), 2670 (s), 2409 (s), 2543 (s), 2033 (s), 1647 (s), 1462 (m), 1377 (m), 1306 (s), 1155 (s), 1075 (s), 1036 (s), 1005 (m), 971 (s), 890 (s), 848 (s), 770 (s), 722 (m) cm^{-1}. Unit cell (Mo Kα, −120 °C): triclinic space group $P\bar{1}$, with a = 11.977(7) Å, b = 12.122(4) Å, c = 20.735(13) Å, α = 99.81(4)°, β = 101.35(5)°, γ = 114.88(4)°, and V = 2567(3) $Å^3$.

Synthesis of $(THF)_{10}Yb_6Se_6I_6\cdot THF$ (5). Yb (0.284 g, 1.64 mmol), PhSSPh (0.358 g, 1.64 mmol), and I_2 (0.208 g, 0.820 mmol) were combined in THF (30 mL) and stirred until the metal was consumed (1 day). Elemental Se (0.131 g, 1.66 mmol) was added, and after 1 day, the deep red solution was filtered away from brown precipitate and layered with hexane (20 mL) to give red-brown crystals (0.429 g, 51%) that turn black at 230 °C. IR: 2917 (s), 2856 (s), 1461 (s), 1377 (s), 1306 (w), 1261 (w), 1168 (w), 1155 (w), 1077 (w), 1035 (w), 1006 (m), 916 (w), 888 (w), 1852 (m), 771 (w), 736 (m), 724 (m), 689 (w), 668 (w) cm^{-1}. UV−vis (THF): λ_{max} = 381 nm (200 M^{-1} cm^{-1}). Anal. Calcd for $C_{44}H_{88}I_6O_{11}Se_6Yb_6$: C, 17.2; H, 2.89. Found: C, 17.5; H, 3.02.

Thermolysis. Crystalline compounds were sealed in evacuated quartz tubes and heated at 700 °C for 6 h, with a portion of the

(6) (a) Kern, R. J. *J. Am. Chem. Soc.* **1953**, *75*, 1865. (b) Peach, M. E. *J. Inorg. Nucl. Chem.* **1973**, *35*, 1046. (c) Peach, M. E. *J. Inorg. Nucl. Chem.* **1979**, *41*, 1390.

(7) Melman, J. H.; Fitzgerald, M.; Freedman, D.; Emge, T. J.; Brennan, J. G. *J. Am. Chem. Soc.* **1999**, *121*, 10247.

Table 1. Summary of Crystallographic Details for **1** and **5**

	1	**2**	**5**
empirical formula	$C_{28}H_{56}I_2O_7Se_9Yb_4$	$C_{28}H_{56}I_2O_7Se_9Tm_4$	$C_{20}H_{40}I_3O_5Se_3Yb_3$
fw	2161.33	2144.89	1497.22
space group	*C*2/*c*	$P\bar{1}$	$P2_1/n$
a (Å)	19.973(5)	11.897(8)	11.960(3)
b (Å)	13.052(4)	12.008(3)	14.412(2)
c (Å)	38.85(2)	20.582(5)	19.886(6)
α (deg)	90.00	97.72(3)	90.00
β (deg)	90.59	103.52(50	91.49(5)
γ (deg)	90.00	114.78(3)	90.00
V (Å^3)	10 127(7)	2504(1)	3427(1)
Z	8	2	4
D (calcd) (g/cm^{-3})	2.835	2.845	2.902
T (°C)	−120	−120	−120
λ (Å)	0.710 73	0.710 73	0.717 03
abs coeff (mm^{-1})	15.043	14.826	14.003
$R(F)^a$ [$I > 2\sigma(I)$]	0.065	0.040	0.052
$R_w(F^2)^a$ [$I > 2\sigma(I)$]	0.143	0.115	0.085

[a] Definitions: $R(F) = \sum||F_o| - |F_c||/\sum|F_o|$; $R_w(F^2) = \{\sum[w(F_o^2 - F_c^2)^2]/\sum[w(F_o^2)^2]\}^{1/2}$. Additional crystallographic details are given in the Supporting Information.

tube remaining outside the oven, submerged in liquid nitrogen to collect liberated THF. X-ray powder diffraction identified Yb_2Se_3[8] and Er_2Se_3[9] as the only crystalline solid-state products resulting from the thermolysis of **1** and **3**, respectively.

X-ray Structure Determination of 1, 2, and 5. Single-crystal X-ray diffraction data for **1**, **2**, and **5** were collected on a Nonius CAD4 diffractometer with graphite monochromatized Mo Kα radiation (λ = 0.710 73 Å) at −120 °C. The check reflections measured every hour showed less than 3% intensity variation. The data were corrected for Lorentz effects and polarization and for absorption, the latter by a numerical (SHELX76)[10] method. The structures were solved by Patterson or direct methods (SHELXS86).[11] All non-hydrogen atoms were refined (SHELXL97) on the basis of F_{obs}^2. All hydrogen atom coordinates were calculated with idealized geometries (SHELXL97).[12] Scattering factors (f_o, f', f'') are as described in SHELXL97. Crystallographic data and final *R* indices for **1**, **2**, and **5** are given in Table 1. Significant bond distances and angles for **5** are given in Table 2, while significant distances for **1** and **2** are given in Figure 1. Complete crystallographic details are given in the Supporting Information. An ORTEP diagram[13] for the common structural framework of **1** and **2** is shown in Figure 1, and an ORTEP diagram for **5** is given in Figure 2.

Table 2. Significant Distances (Å) and Angles (deg) for **5**[a]

Distances

Yb(1)−O(2)	2.31(1)	Yb(1)−O(1)	2.309(12)	Yb(1)−Se(1)	2.730(2)
Yb(1)−Se(2)	2.750(2)	Yb(1)−Se(3)	2.817(2)	Yb(1)−I(2)	2.967(2)
Yb(2)−O(3)	2.29(1)	Yb(2)−O(4)	2.32(1)	Yb(2)−Se(1)	2.746(2)
Yb(2)−Se(2)	2.785(2)	Yb(2)−Se(3)′	2.788(2)	Yb(2)−I(1)	2.974(2)
Yb(3)−O(5)	2.32(1)	Yb(3)−Se(1)	2.755(2)	Yb(3)−Se(2)′	2.765(2)
Yb(3)−Se(3)	2.834(2)	Yb(3)−Se(3)′	2.857(2)	Yb(3)−I(3)	2.977(2)

Angles

O(2)−Yb(1)−O(1)	79.5(5)	O(2)−Yb(1)−Se(1)	94.9(3)
O(1)−Yb(1)−Se(1)	174.3(3)	O(2)−Yb(1)−Se(2)	171.8(3)
O(1)−Yb(1)−Se(2)	95.2(3)	Se(1)−Yb(1)−Se(2)	90.16(7)
O(2)−Yb(1)−Se(3)	86.3(3)	O(1)−Yb(1)−Se(3)	88.5(3)
Se(1)−Yb(1)−Se(3)	89.71(7)	Se(2)−Yb(1)−Se(3)	87.27(7)
O(2)−Yb(1)−I(2)	88.5(3)	O(1)−Yb(1)−I(2)	88.9(3)
Se(1)−Yb(1)−I(2)	92.40(6)	Se(2)−Yb(1)−I(2)	97.72(6)
Se(3)−Yb(1)−I(2)	174.58(6)	O(3)−Yb(2)−O(4)	84.8(5)
O(3)−Yb(2)−Se(1)	93.7(4)	O(4)−Yb(2)−Se(1)	176.4(3)
O(3)−Yb(2)−Se(2)	92.1(4)	O(4)−Yb(2)−Se(2)	87.6(3)
Se(1)−Yb(2)−Se(2)	89.10(7)	O(3)−Yb(2)−Se(3)′	175.7(4)
O(4)−Yb(2)−Se(3)′	91.7(3)	Se(1)−Yb(2)−Se(3)′	89.90(7)
Se(2)−Yb(2)−Se(3)′	90.19(7)	O(3)−Yb(2)−I(1)	86.9(4)
O(4)−Yb(2)−I(1)	88.8(3)	Se(1)−Yb(2)−I(1)	94.45(7)
Se(2)−Yb(2)−I(1)	176.38(6)	Se(3)′−Yb(2)−I(1)	90.53(7)
O(5)−Yb(3)−Se(1)	90.4(3)	O(5)−Yb(3)−Se(2)′	91.3(3)
Se(1)−Yb(3)−Se(2)′	174.35(7)	O(5)−Yb(3)−Se(3)	177.6(3)
Se(1)−Yb(3)−Se(3)	88.85(7)	Se(2)′−Yb(3)−Se(3)	89.63(7)
O(5)−Yb(3)−Se(3)′	94.8(3)	Se(1)−Yb(3)−Se(3)′	88.32(7)
Se(2)′−Yb(3)−Se(3)′	86.18(7)	Se(3)−Yb(3)−Se(3)′	87.46(6)
O(5)−Yb(3)−I(3)	82.8(3)	Se(1)−Yb(3)−I(3)	92.71(6)
Se(2)′−Yb(3)−I(3)	92.84(6)	Se(3)−Yb(3)−I(3)	94.97(5)
Se(3)′−Yb(3)−I(3)	177.37(6)	Yb(1)−Se(1)−Yb(2)	90.94(7)
Yb(1)−Se(1)−Yb(3)	92.35(7)	Yb(2)−Se(1)−Yb(3)	92.39(7)
Yb(1)−Se(2)−Yb(3)′	94.99(7)	Yb(1)−Se(2)−Yb(2)	89.73(7)
Yb(3)′−Se(2)−Yb(2)	90.74(6)	Yb(2)′−Se(3)−Yb(1)	177.97(9)
Yb(2)′−Se(3)−Yb(3)	89.26(6)	Yb(1)−Se(3)−Yb(3)	88.90(7)
Yb(2)′−Se(3)−Yb(3)′	89.39(7)	Yb(1)−Se(3)−Yb(3)′	91.56(7)
Yb(3)−Se(3)−Yb(3)′	92.54(6)		

[a] Symmetry transformations used to generate equivalent atoms: (′) $-x + 1, -y, -z$.

Results

Selenium rich lanthanide clusters with ancillary iodide ligands can be isolated for both redox active Yb and the larger lanthanides Tm, Ho, and Er. Reduction of PhSeSePh/I_2 mixtures with elemental Ln is facile at room temperature in the presence of trace mercury catalyst (reaction 1), and the resultant SePh anions are readily oxidized by Se to give $(THF)_6Yb_4I_2(SeSe)_4(\mu_4\text{-Se})$ (Ln = Yb(**1**), Tm(**2**), Er(**3**), Ho(**4**)) in ∼20% yield. Low-temperature single-crystal X-ray diffraction experiments on **1**, **2**, and **4** reveal that the products crystallize in two different unit cells; complete structural analyses of **1** and **2** were obtained, and the unit cell of **4** was found to be nearly identical to that of **2**. Figure 1 gives an ORTEP diagram of the common structural framework for **1** and **2**, and significant distances and angles for **1** and **2** can be found in the figure caption. In the structures of **1** and

(8) Dismukes, J. P.; White, J. G. *Inorg. Chem.* **1965**, *4*, 970.
(9) Guittard, M.; Benacerraf, A.; Flahaut, J. *Ann. Chim.* **1964**, *9*, 25.
(10) Sheldrick, G. M. *SHELX76, Program for Crystal Structure Determination*; University of Cambridge: Cambridge, U.K., 1976.
(11) Sheldrick, G. M. *SHELXS86, Program for the Solution of Crystal Structures*; University of Göttingen: Göttingen, Germany, 1986.
(12) Sheldrick, G. M. *SHELXL97, Program for Crystal Structure Refinement*; University of Göttingen: Göttingen, Germany, 1997.
(13) (a) Johnson, C. K. *ORTEP II*; Report ORNL-5138; Oak Ridge National Laboratory: Oak Ridge, TN, 1976. (b) Zsolnai, L. *XPMA and ZORTEP, Programs for Interactive ORTEP Drawings*; University of Heidelberg, Heidelberg, Germany, 1997.

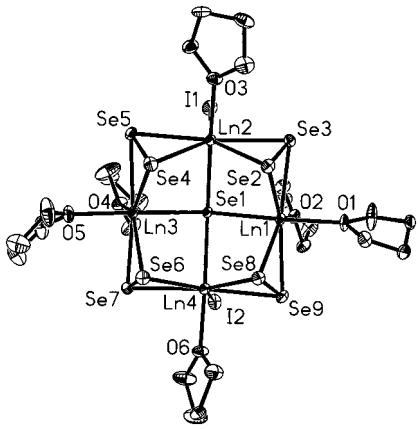

Figure 1. Molecular structure of $(THF)_6Ln_4I_2(SeSe)_4(\mu\text{-Se})$ [Ln = Yb (**1**), Tm (**2**)]. These compounds crystallize in two different unit cells that differ in the orientation of the lattice solvents, but the core cluster structure is the same. Thermal ellipsoids (for **1**) are drawn at the 50% probability level. Significant distances (Å) for **1**: Yb(1)−O(1), 2.27(1); Yb(1)−O(2), 2.28(1); Yb(1)−Se(8), 2.779(2); Yb(1)−Se(1), 2.808(2); Yb(1)−Se(2), 2.808(3); Yb(1)−Se(3), 2.821(3); Yb(1)−Se(9), 2.822(3); Yb(2)−O(3), 2.30(1); Yb(2)−Se(3), 2.804(3); Yb(2)−Se(5), 2.808(3); Yb(2)−Se(4), 2.821(3); Yb(2)−Se(2), 2.839(2); Yb(2)−Se(1), 2.863(2); Yb(2)−I(1), 2.977(2); Yb(3)−O(5), 2.27(1); Yb(3)−O(4), 2.31(1); Yb(3)−Se(4), 2.782(3); Yb(3)−Se(1), 2.794(2); Yb(3)−Se(6), 2.799(2); Yb(3)−Se(5), 2.833(3); Yb(3)−Se(7), 2.836(3); Yb(4)−O(6), 2.31(1); Yb(4)−Se(7), 2.812(2); Yb(4)−Se(9), 2.818(2); Yb(4)−Se(8), 2.825(2); Yb(4)−Se(6), 2.844(3); Yb(4)−Se(1), 2.873(2); Yb(4)−I(2), 2.968(2); Se(2)−Se(3), 2.372(3); Se(4)−Se(5), 2.377(3); Se(6)−Se(7), 2.372(4); Se(8)−Se(9), 2.379(3). Significant distances (Å) for **2**: Tm(1)−O(1), 2.274(7); Tm(1)−O(2), 2.300(7); Tm(1)−Se(2), 2.784(2); Tm(1)−Se(1), 2.812(1); Tm(1)−Se(8), 2.822(2); Tm(1)−Se(9), 2.825(2); Tm(1)−Se(3), 2.840(2); Tm(2)−O(3), 2.327(7); Tm(2)−Se(5), 2.817(2); Tm(2)−Se(2), 2.837(2); Tm(2)−Se(3), 2.837(2); Tm(2)−Se(4), 2.857(2); Tm(2)−Se(1), 2.874(2); Tm(2)−I(1), 2.980(2); Tm(3)−O(5), 2.288(8); Tm(3)−O(4), 2.320(8); Tm(3)−Se(1), 2.799(2); Tm(3)−Se(6), 2.804(1); Tm(3)−Se(4), 2.816(2); Tm(3)−Se(5), 2.845(2); Tm(3)−Se(7), 2.850(2); Tm(4)−O(6), 2.290(7); Tm(4)−Se(9), 2.802(2); Tm(4)−Se(7), 2.823(2); Tm(4)−Se(6), 2.840(3); Tm(4)−Se(8), 2.854(2); Tm(4)−Se(1), 2.868(1); Tm(4)−I(2), 2.991(2); Se(2)−Se(3), 2.386(2); Se(4)−Se(5), 2.379(2); Se(6)−Se(7), 2.382(2); Se(8)−Se(9), 2.374(2).

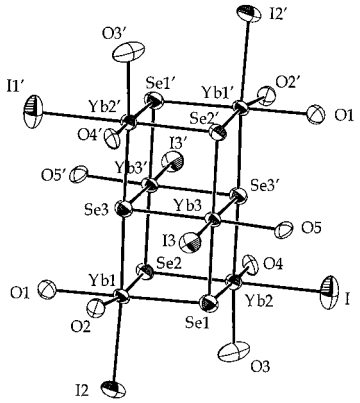

Figure 2. Molecular structure of $(THF)_{10}Yb_6Se_6I_6$, with the C and H atoms removed for clarity. Thermal ellipsoids are drawn at the 50% probability level.

2, a single Se^{2-} ligand lies above the Ln_4 plane (0.79 Å), and the two terminal iodide ligands coordinate nonadjacent Ln on the opposite side of the Ln_4 plane. There are four SeSe ligands bridging the sides of the Ln_4 square, with a strikingly narrow range of Se−Se bond lengths (i.e., 2.372(2)−2.379(2) Å in **1**). There are two chemically inequivalent Ln atoms per structure, with distinctly different Ln−Se bond lengths. For example, in **1**, bonds from Yb to the SeSe ligands are slightly longer when the Yb is coordinated to iodide ($Yb(1)-Se_{avg}$ = 2.808 Å, $Yb(3)-Se_{avg}$ = 2.813 Å; $Yb(2)-Se_{avg}$ = 2.818 Å, and $Yb(4)-Se_{avg}$ = 2.825 Å), and there is a more dramatic elongation in bond lengths between Yb and the central μ_4-Se(1) ligand, with the (I)Yb−Se bonds longer by ∼0.06 Å (2.873(2) Å, 2.863(2) Å) than the Yb−Se bonds (2.808(2) Å, 2.794(2) Å). Identical trends are noted in **2**.

$$4Ln + I_2 + PhSeSePh \rightarrow 4\text{“}LnI_{0.5}(SePh)_{2.5}\text{”} \xrightarrow{9Se} (THF)_6Yb_4I_2(SeSe)_4(\mu_4\text{-Se}) \quad (1)$$

The Tm, Ho, and Er derivatives are yellow, suggesting that the color is related to the SeSe ligand, rather than to an intrinsic property of the metal. The redox active Yb compound **1** is intensely colored, with a relatively broad absorption band in the visible spectrum at 387 nm that can be assigned as a Se to Yb charge transfer absorption. These compounds decompose thermally to give Ln_2Se_3 (reaction 2), with the elimination of Se. The iodide containing product was not identified, but X-ray fluorescence measurements of the sublimed solid state thermolysis product indicates that there is significant Yb deposition in the cold zone of the thermolysis experiment, and there is no iodide remaining in the nonvolatile solid-state product.

$$(THF)_6Ln_4I_2(SeSe)_4(\mu_4\text{-Se}) \rightarrow Ln_2Se_3 + Se + THF + ?? \quad (2)$$

In the absence of excess Se, diselenido linkages do not form. The Yb compound $(THF)_{10}Yb_6Se_6I_6$ (**5**) was prepared by the stoichiometric reaction of “$YbI(SPh)_2$” with one Se, and it crystallizes in ∼50% yield. Low-temperature single-crystal X-ray diffraction analysis reveals that the product is a double cubane, with one face of a Yb_4Se_4 cube capped by an additional Yb_2Se_2 layer. Figure 2 gives an ORTEP diagram of the molecular structure for **5**, and significant bond lengths and angles for **5** are given in Table 2. All six octahedral Yb(III) ions have a terminal iodide ligand, and THF donors occupy the remaining coordination sites, with two THF molecules per external Yb [Yb(1), Yb(2)] and one coordinating the pair of internal [Yb(3)] ions.

Bond lengths in **5** depend on geometry. Looking first at the μ_4-Se^{2-} ligand, there are essentially four different Yb−Se bonds that can be divided into two sets: a nearly linear pair [Se(3)−Yb(1), 2.817(2) Å; Se(3′)−Yb(2), 2.788(2) Å] that is clearly longer than the set of orthogonal bonds [Se(3)−Yb(3), 2.834(2) Å; Se(3)−Yb(3′), 2.857(2) Å]. Within the linear and orthogonal pair, there are two distinct types: Yb−Se bonds trans to iodide ligands and Yb−Se bonds trans to THF ligands. In each pair, the bond trans to the I^- is longer than the bond trans to the THF ligand, by approximately 0.025 Å.

The μ_3-Se^{2-} ligands can be analyzed similarly. There are three μ_3-Se^{2-} bonds in **5** that are trans to THF [Yb(1)−Se(2), 2.750(2) Å; Yb(1)−Se(1), 2.730(2) Å; Yb(2)−Se(1), 2.746(2) Å], only one Yb−Se bond trans to an iodide ligand

[Yb(2)−Se(2), 2.785(2) Å], and two bonds trans to selenido ligands [Yb(3)−Se(1), 2.755(2) Å; Yb(3′)−Se(2), 2.765(2) Å]. As found in the μ_4-Se^{2-} bond length data, the Yb−Se bond trans to I^- is the longest (by an average of 0.037 Å relative to the average of the bonds trans to THF); the Yb−Se bonds trans to selenido ligands are slightly shorter than those trans to I^- but longer than the bonds trans to THF, and Yb−Se bonds trans to THF are the shortest in the cluster.

Discussion

Selenium rich compounds **1**−**4** are distinctly related to their sulfido analogues, suggesting that this Ln_4 framework is a particularly stable arrangement for chalcogen rich compounds. The Yb compound **1** has the same space group and molecular structure as $(THF)_6Yb_4I_2S_9$,[7] and the Tm compound **2** has the same cluster framework, with a lower lattice symmetry but nearly identical molecular and crystal packing features, including the location of the THF of solvation directly above the Se_8 "crown". The Ho derivative **4** has the same unit cell as **2**.

In contrast, these iodo clusters differ structurally from their selenium rich chalcogenolate counterparts.[14] Clusters **1**−**4** have structures that resemble "$(py)_8Yb_4Se_8(Se)(EPh)_2$" (E = Se, Te), but the relative strength of Yb−I and Yb−E(Ph) bonds has a dramatic influence on product structure. In particular, in "$(py)_8Yb_4Se_8(Se)(SePh)_2$", a selenolate ligand is actually displaced from the Yb coordination sphere and instead coordinates to a SeSe unit, forming a SeSeSePh moiety. The tellurolate compound is even more complicated, because there is both displacement of TePh/coordination to SeSe, as well as insertion of a Se atom into the remaining Yb−Te bond to form a terminal SeTePh ligand. Because the Yb−I bond is stronger than either Yb−E(Ph) bond, iodide is not displaced from a Ln coordination sphere, does not coordinate to SeSe, and does not react with Se to form an insertion product. The iodide simply remains coordinated to the Ln.

Cluster **5** is structurally related to the sulfido double cubane $(py)_{10}Yb_6S_6(SPh)_6$,[5e] although it differs significantly in the distribution of ancillary SPh/I ligands. In **5**, there is a terminal I^- coordinated to each Yb, whereas in the sulfido cluster, the SPh ligands were all found on the external Yb, with only pyridine and S^{2-} coordinating to the internal Yb. This reorganization of ancillary ligands is presumably a mechanism for reducing ligand−ligand repulsions in the thiolate compound.

The difference in nuclearity between $(py)_8Yb_4Se_4(SePh)_4$ and $(py)_{10}Yb_6S_6(SPh)_6$ had been attributed to the difference in chalcogenido basicity, with the stronger sulfido donor forming the product with both μ_3 and μ_4 chalcogenido ligands.[5e] Clearly, the structure of **5** indicates that chalcogenido basicity is not the only variable governing product nuclearity. Relative basicity can still explain the different structures of **5** and $(py)_8Yb_4Se_4(SePh)_4$, because in this pair, the larger cluster crystallizes from the weaker Lewis base solvent THF, and the stronger pyridine donor more effectively interrupts bridging chalcogenido interactions to form the tetrametallic product.

Directional bonding is not traditionally associated with lanthanide chemistry, but there are now a number of octahedral chalcogenolate compounds[15] and chalcogenido cluster compounds[5e] with Ln−E bond lengths that are clearly influenced by the identity of the trans ligand. The effects are generally on the order of 0.02−0.05 Å, with a "trans" lengthening order: THF, py < EPh < E^{2-} < I. Preliminary calculations on model systems do not point to a well-defined "covalent" origin of these effects, and additional examples are currently targeted to help explain the observed trends.

The electronic spectrum of the halogenated cluster $(THF)_6Yb_4I_2(SS)_4(\mu_4\text{-}S)$ was unusually well defined, such that two low energy absorptions at 420 and 457 nm could be resolved. These absorptions were assigned as LMCT transitions originating with the S^{2-} and SS^{2-} ligands. The color was clearly related to the redox activity of the Yb ion, because the analogous $(THF)_6Tm_4I_2(SS)_4(\mu_4\text{-}S)$ cluster was colorless, as is characteristic for Tm(III). Electronic spectra of $Yb_4Se_9(EPh)_2$ (E = S, Se, Te)[14] were more complicated; only a single, broader absorption could be resolved for the tellurolate compound (λ_{max} = 381 nm in pyridine; λ_{max} = 370 nm in THF), whereas there were two resolved absorptions in both the selenolate derivative (λ_{max} = 351, 500 nm) and thiolate compound (λ_{max} = 380, 445 nm). In the present system, the SeSe linkage dominates the electronic properties of **2**−**4**, which are all yellow because of an allowed π_g to σ_u transition,[16] as is found in main group compounds with SeSe ligands.[17] The intense red colors of **1** and **5** can again be attributed to Se to Yb charge-transfer processes.

Thermolysis of these iodo compounds could yield one of several products, that is, Ln_2Se_3, mixtures of LnI_3/Ln_2Se_3, or LnSeI. In theory, iodide compounds should be preferred products, both because iodine is more electronegative than Se and iodide is not displaced from Ln coordination spheres in reactions of $LnI_x(EPh)_{3-x}$ with elemental Se in Lewis base solvents. Nevertheless, both of the Se rich compounds **1** and **3** yielded only crystalline Ln_2Se_3, as determined by X-ray powder diffraction measurements, and no I^- was detected in the nonvolatile thermolysis product. Iodide was detected in the inorganic products that condensed outside the furnace, but discrete iodide containing products could not be identified. X-ray fluorescence revealed a continuous range of Ln/Se/I compositions that show I/Ln and I/Se ratios increasing along with the distance from the heating source, as might be expected given the utility of iodine as a transport reagent in solid-state syntheses.

(14) Kornienko, A.; Emge, T.; Brennan, J. *J. Am. Chem. Soc.* **2001**, *123*, 11933.

(15) (a) Lee, J.; Brewer, M.; Berardini, M.; Brennan, J. *Inorg. Chem.* **1995**, *34*, 3215. (b) Aspinall, H. C.; Cunningham, S. A.; Maestro, P.; Macaudiere, P. *Inorg. Chem.* **1998**, *37*, 5396. (c) Mashima, K.; Nakayama, Y.; Fukumoto, H.; Kanehisa, N.; Kai, Y.; Nakamura, A. *J. Chem. Soc., Chem. Commun.* **1994**, 2523.

(16) Schlaich, H.; Lindner, G.-G.; Feldmann, J.; Göbel, E. O.; Reinen, D. *Inorg. Chem.* **2000**, *39*, 2740.

(17) (a) Ansari, M. A.; Ibers, J. A.; O'Neal, S. C.; Pennington, W. T.; Kolis, J. W. *Polyhedron* **1992**, *11*, 1877. (b) Smith, D. M.; Pell, M. A.; Ibers, J. A. *Inorg. Chem.* **1998**, 37, 2340.

Conclusion

Lanthanide selenido clusters with ancillary iodide ligands can be isolated either as cubane-like materials or as selenium rich compounds with SeSe ligands by adjusting relative Ln/Se/I starting ratios. The Yb−Se bonds in the cubane cluster have bond lengths that are geometry dependent. The Se rich compounds are useful as single source precursors to Ln_2Se_3 because C−Se bond cleavage is not part of the thermolysis process.

Acknowledgment. This work was supported by the National Science Foundation under Grant CHE-9982625.

Supporting Information Available: X-ray crystallographic files in CIF format for the crystal structures of **1**, **2**, and **5** are available. This material is available free of charge via the Internet at http://pubs.acs.org.

IC010740O